ISBN: 978-3-95450-219-6 ISSN: 2226-0366 doi: 10.18429/JACoW-LINAC2024-THPB095

DESIGN AND SIMULATION OF VIRTUAL PEPPER-POT METHOD FOR LOW ENERGY PROTON BEAM

E. Cosgun*, M. S. Hur, Ulsan National Institute of Science and Technology, Ulsan, South Korea
S. Moon, D. Kim, Korea Multipurpose Accelerator Complex, Gyeongju, South Korea
M. Chung, Pohang University of Science and Technology, Pohang, South Korea

Abstract

The Virtual Pepper-Pot (VPP) is a 4D transverse phase space measurement technique based on pepper-pot-like patterns that are generated by crossing each measured horizontal slit-based beamlet with all measured vertical slit-based beamlets. The VPP beam phase space distribution reconstruction and simulation are performed using the Beam Delivery Simulation (BDSIM) code, which is a Geant4 toolkit. The configuration includes a VPP 3D model slit, a scintillator screen, and a user-defined 1 MeV energy and 10 mA current proton beam distribution, characteristic of the KOMAC RFQ beam test stand. Besides VPP, pepper-pot mask simulation is carried out, and the intensity and emittance differences are observed. The input beam distribution is generated from a TraceWin output file for comparison of results. The comparison between the VPP analysis results and the TraceWin input shows satisfactory results, ensuring accurate estimation of the emittance.

INTRODUCTION

The measurement and analysis of transverse phase space in particle beams are vital for optimizing accelerator performance and improving beam quality. Traditional techniques, such as slit-based and pepper-pot methods, have been widely used for these measurements. Besides these, the Virtual Pepper-Pot (VPP) technique has been developed to achieve high resolution and to provide fast scanning, offering a novel approach to 4D transverse phase space measurements.

The VPP technique generates pepper-pot-like patterns by crossing horizontal slit-based beamlets with vertical slit-based beamlets, providing a comprehensive view of the beam's phase space distribution [1]. This method is implemented using the Beam Delivery Simulation (BDSIM) code [2], a sophisticated simulation tool based on the Geant4 [3] toolkit. BDSIM allows to simulate both the transport of particles in an accelerator and their interaction with the accelerator material.

A key application of the VPP technique is its use in the Korea Multi-purpose Accelerator Complex (KOMAC) Radio Frequency Quadrupole (RFQ) beam test stand. Here, a user-defined proton beam distribution with 1 MeV energy and 10 mA current is employed. The simulation configuration includes a 3D model slit and a scintillator screen, considering the main beam parameters of test stand.

To validate the VPP method, simulations are compared with traditional pepper-pot mask techniques. These comparisons focus on intensity and emittance differences, providing insights into the advantages of VPP over conventional methods. Additionally, the input beam distribution is generated from a TraceWin output file, allowing for a direct comparison between VPP analysis results and TraceWin inputs. The satisfactory agreement between these results highlights the accuracy and reliability of the VPP technique in estimating emittance.

This paper aims to present a comprehensive overview of the VPP technique, its construction, and its validation through comparative analysis.

* emrecosgun@unist.ac.kr

KOMAC BEAM TEST STAND LAYOUT

Radio-Frequency Quadrupole Beam Test Stand (BTS) is a proton accelerator structure at Korea Multipurpose Accelerator Complex (KOMAC) that accelerates beams to 1 MeV/n. In addition to the microwave ion source, an LEBT, and an RFQ, the BTS consists of two beamlines, each with triple quadrupole magnets and a wire scanner. A detailed ion source extraction simulation study [4] shows that beams are transmitted to LEBT with 25 keV energy and 10~15 mA current.

There are two beamlines at the KOMAC BTS, one of which has a straight beamline (BL1) and another consisting of a bending magnet at 30°. Since the phase space measurement will be carried out BL1 in this study we will focus on this beamline. The BL1 features four small quadrupoles immediately after the RFQ and has a triplet quadrupole structure to optimize beam transportation to the target chambers by adjusting the quadrupole gradients. The TraceWin code [5] shows that the beam distribution from RFQ exit is fully transmitted to diagnostic chamber. Figure 1 gives the RMS beam trajectories along the beamline, and the horizontal and vertical phase space distributions at the measurement point are given in Fig. 2.

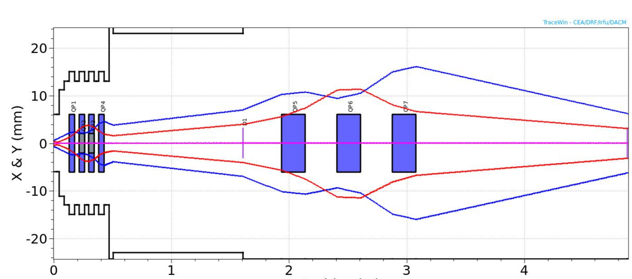

Figure 1: KOMAC BTS straight beam line envelope simulation. Blue line indicates x axis while red shows y axis.

ISBN: 978-3-95450-219-6 ISSN: 2226-0366 doi: 10.18429/JACoW-LINAC2024-THPB095

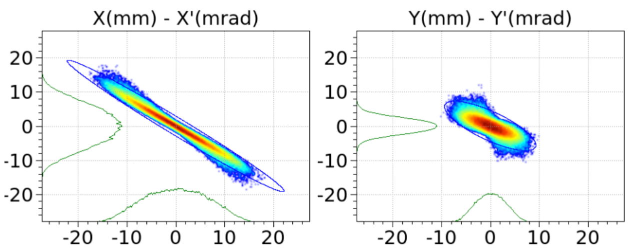

Figure 2: Beam phase space distributions at end of the beamline where diagnostic chamber is located.

DESIGN AND SIMULATION

Thickness of the Slit

When it comes to calculating damage levels, slit protection systems are usually conservatively designed and operated. It is therefore useful to have a general understanding of energy deposition characteristics for typical materials such as tungsten and graphene. Since the range of a particle in a material is the distance it travels before coming to rest and has the following relation of the deposited energy [6]:

$$R = \int_{E_0}^{0} \frac{dE}{dE/dx} \tag{1}$$

Figure 3 shows the energy deposition distribution, which is numerically calculated in Geant4 code, corresponding to a beam energy of 1 MeV which is accelerated beam at RFQ. Considering this energy level, the proton releases its majority of energy in the target around $R = 5.3\ \mu$m and $R = 12.5\ \mu$m for tungsten and graphene material, respectively, implying the presence of the Bragg peak. Based on this calculation, determining the slit thickness $L = 0.1$ mm is reliable for our operation.

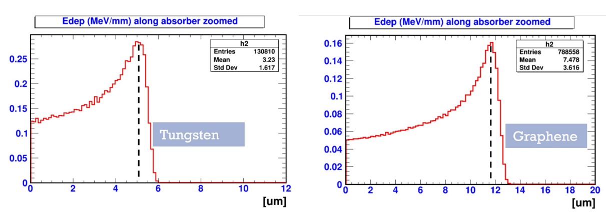

Figure 3: Simulations to study the penetration of proton beam into tungsten and graphene blocks.

Analytic Consideration

After determining the slit width (d), the angular acceptance of the slits can be assessed by considering the selected slit depth (L). We can consider the uncorrelated angles must be chosen to be less than one-fourth the angular aperture of the slits, $\phi < d/4L$ and preferably even smaller [7]. Trajectory simulation shows that the rms beam angle at the target is varied between 2 mrad and 5 mrad. Based on this output the slit width is taken to be 0.2 mm. The slit separation (w), in our case slit step size, should be much larger than the slit width d and smaller than the beam size to ensure that the beam can be resolved. Perpendicular slit separation (s) is larger than at least 2 times rms beam width to prevent overlapping the beam on the screen. General layout of the slit is illustrated in Fig. 4. The dimensions are designed as much as large, taking into account the size of the vacuum chamber port. In this case the s value is calculated around 40 mm which is much larger than 6 mm rms size beam.

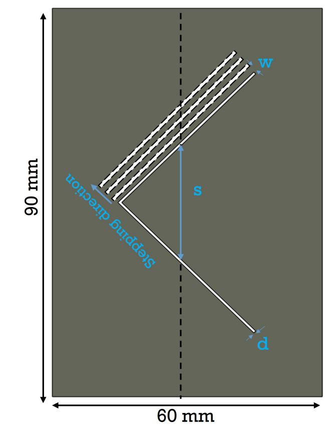

Figure 4: The layout of VPP with it's dimensions.

Data Construction

The first step of the numerical simulation of the phase space measurement is defining the configuration in BDSIM. The 3D model of slit shown in Fig. 4 is imported to BDSIM and scintillator screen is defined 0.11 m downstream of the slit. The output phase space distribution of TraceWin which is given in Fig. 2 is used as input distribution to validate the results. Figure 5 gives the concept of the phase space construction method. The slit is oriented diagonally at a 45° angle to the horizontal plane and is stepping in that direction. For every stepping position 1 million *event* are created and the projection of beamlets on screen is saved. It is noted that both horizontal and vertical slits capture all beams, and no intersection point is encountered during scanning. For each pixel, the minimum value to be used is calculated from both beamlets $min(f_x, f_y)$, and a pepper-pot-like image is created, as shown in the figure.

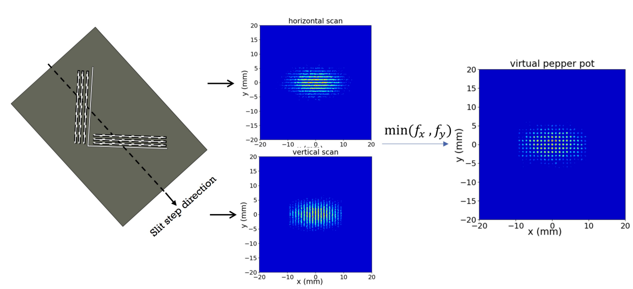

Figure 5: Construction method of pepper-pot-like image from VPP.

Moreover, 3D model pepper-pot mask is positioned 0.11 meters beyond the target, which consisted of a 49 × 49 array of holes, each 0.2 mm in diameter with a 2 mm interval. The

ISBN: 978-3-95450-219-6 ISSN: 2226-0366 doi: 10.18429/JACoW-LINAC2024-THPB095

beamlet projection is saved on the screen using the same settings and *event* as before. Figure 6 displays the VPP and pepper-pot images. It is apparent that the VPP shows higher intensity projections.

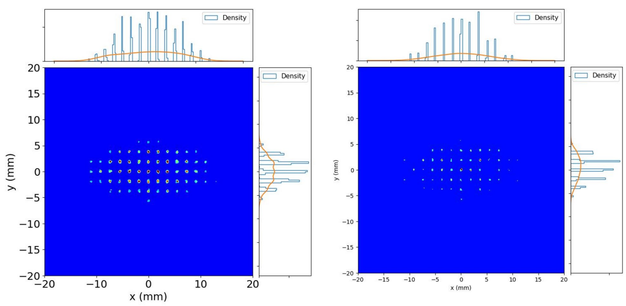

Figure 6: On the left, constructed virtual pepper-pot image, and on the right, a projection of the pepper-pot image.

The projection information is used to calculate the emittance values based on the moments of the beamlets and their relative intensities. Based on the offsets between beamlet position and crossed slit (or hole) position and the intensity distributions of the beamlets, phase space distributions are reconstructed which is shown in Fig. 7. Table 1 shows the results of VPP and pepper-pot phase space distributions, as well as the relative errors to TraceWin. The maximum error rate is calculated to be approximately 2% for both methods in the phase space.

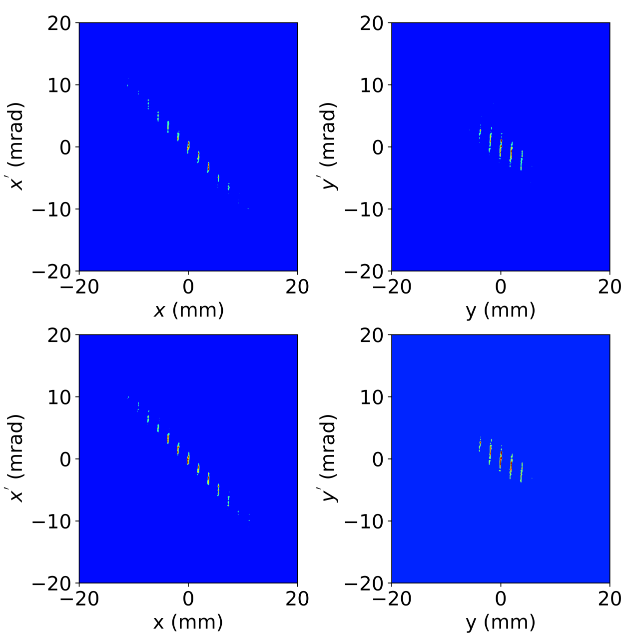

Figure 7: Both horizontal and vertical phase space distributions of pepper-pot (top) and VPP (bottom).

EXPERIMENTAL SETUP

The experimental setup mainly includes a VPP along with pepper-pot actuators and slits positioned at a 45° angle to the horizontal axis within the chamber, and a scintillator screen situated 0.11 m downstream of the slit plane. The experimental layout is shown in Fig. 8. A Basler-type camera will be utilized to capture high-resolution images. Additionally, a wire scanner is employed to observe the center of the beam prior to the experiment.

Table 1: Results of Constructed Phase Space Distributions and Relative Error Rate To Input Beam Distribution

	$\varepsilon_{x,norm}$ **(mm mrad)**	$\varepsilon_{y,norm}$ **(mm mrad)**	$\Delta\epsilon_x$ **(%)**	$\Delta\epsilon_y$ **(%)**
Tracewin	0.230	0.190	-	-
VPP	0.235	0.188	2.17	1.01
Pepper-pot	0.233	0.194	1.30	2.10

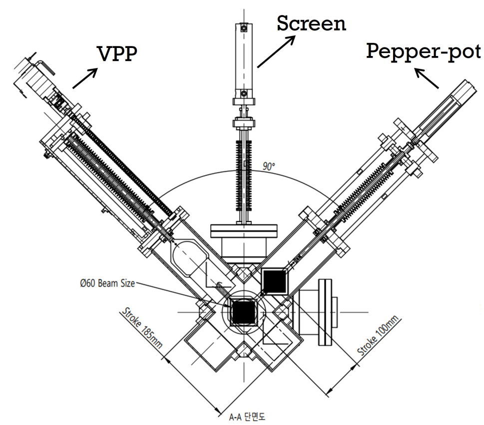

Figure 8: Experimental configuration which includes both pepper-pot and VPP mask.

CONCLUSION

An analytical model and numerical simulation are discussed to construct a virtual pepper-pot method and to determine the horizontal and vertical phase space for 4D transverse beam distribution. We discussed in detail the proof-of-principle simulations performed on BDSIM generated beams, and compare the pepper-pot results with the VPP 4D phase space simulations to quantify the systematic error of the technique. The experimental setup provides an opportunity to compare the outputs of the VPP and pepper-pot, as both are positioned on the same longitudinal plane.

REFERENCES

[1] G. Georgiev, M. Krasilnikov, *et al.*, “Virtual pepper-pot technique for 4D phase space measurements”, in *Proc. IBIC’19*, Malmö, Sweden, Sep. 2019, pp. 586–590. `doi:10.18429/JACoW-IBIC2019-WEPP029`

[2] L. J. Nevay *et al.*, “Beam Delivery Simulation: BDSIM - Automatic Geant4 Models of Accelerators”, in *Proc. IPAC’16*, Busan, Korea, Jun. 2016, Busan, Korea, pp. 3098–3100. `doi:10.18429/JACoW-IPAC2016-WEPOY046`

[3] J. Allison *et al.*, “Geant4 developments and applications”, *IEEE Transactions on nuclear science*, vol. 53, no. 1, pp. 270–278, 2006.

ISBN: 978-3-95450-219-6 ISSN: 2226-0366 doi: 10.18429/JACoW-LINAC2024-THPB095

[4] E. Cosgun, S. Moon, D. Kim, and M. Chung, “Studies of space-charge compensation of positive ions by creating time-dependent secondary electrons in low-energy beam transport line”, in *Proc. IPAC'20* , Nashville, TN, USA, Jun. 2024, pp. 201–203. doi:10.18429/JACoW-IPAC2024-MOPC61

[5] D. Uriot, N. Pichoff, *et al.*, “Status of TraceWin code”, in *Proc. IPAC'15,* Richmond, VA, USA, May 2015, pp. 92–94. doi:10.18429/JACoW-IPAC2015-MOPWA008

[6] D. E. Groom and S. Klein, “Passage of particles through matter”, *The European Physical Journal C-Particles and Fields*, vol. 15, no. 1-4, pp. 163–173, 2000.

[7] S. Anderson, J. Rosenzweig, G. LeSage, and J. Crane, “Space-charge effects in high brightness electron beam emittance measurements”, *Physical Review Special Topics-Accelerators and Beams*, vol. 5, no. 1, p. 014 201, 2002.